



Extinction Cross-Section Measurements of *Bacillus globigii* Aerosols

Suzanne C. Walts, Craig A. Mitchell, Michael E. Thomas, and Donald D. Duncan

In a continuing series of experiments designed to determine the spectral extinction cross section of bacterial aerosols, two White cell transmissometers were constructed to obtain stable, long path length measurements. A laser transmissometer at 543 nm was used to calibrate a broadband transmissometer (400–850 nm). Spectral transmittance was measured as a function of particle concentration, and extinction cross sections were calculated. Visible band measurements of *Bacillus globigii* aerosols indicated a slight increase in the extinction cross section with increasing wavelength. The extinction cross section was estimated to be $2.58 (\pm 0.25) \times 10^{-8} \text{ cm}^2$ at the 543-nm wavelength.

INTRODUCTION

The need to detect biological aerosol threats exists both in the open atmosphere and within buildings and other enclosed spaces. Current sensor technologies include mass spectroscopy, immuno-assays, lidar, and infrared radiometry. However, the need for standoff remote sensing and speed for early detection has placed an emphasis on optical techniques. A variety of active and passive optical sensors are being evaluated that require knowledge of the extinction and volume backscatter cross sections as a function of wavelength, particle size, and chemical makeup (growth media variations and different aerosolizing procedures).

It is now being recognized that aerosol lidars will play an important role in the remote detection of biological agents. Of the remote sensors being considered, aerosol lidars have the most mature technology. Information obtained from our measurements is critical to the design of an optimal lidar system. The significance of these measurements is seen

in the expression for the range-resolved received power, $P_{\text{rec}}(R)$, for an aerosol lidar system:

$$P_{\text{rec}}(R) = E e^{-2\beta_{\text{ext}}(R)R} \Omega_{\text{rec}} \sigma_{\text{b}} N(R) \frac{c}{2}. \quad (1)$$

Here,

- E = the source pulse energy,
- β_{ext} = the range-dependent extinction “coefficient” (or the extinction cross section per unit volume; $\beta_{\text{ext}}(R) = C_{\text{ext}} N(R)$, where C_{ext} is the extinction cross section),
- Ω_{rec} = the solid angle subtended by the receiver telescope,
- σ_{b} = the backscatter cross section per solid angle of the target aerosol,
- $N(R)$ = the range-dependent aerosol number concentration, and
- c = the speed of light.

To properly design and characterize the performance of the lidar system, the extinction coefficient and backscatter cross section of various bacterial aerosols as a function of concentration and wavelength must be quantified. Knowledge of the spectral dependence of these optical properties may allow discrimination of biological pathogens from naturally occurring background aerosols such as pollen, haze, and dust.

Past measurements of the anthrax simulant *Bacillus globigii* (*Bg*) have been obtained on films¹ and in short-path, high-concentration aerosols.^{2,3} Although these are useful measurements, the results are more qualitative than quantitative. High concentrations tend to cause particles to agglomerate into clusters that are not representative of actual distributions in the atmosphere. Thus, cross-section measurements are needed on realistic aerosol concentration levels that contain single particles. Unfortunately, the transmission losses for propagation through such distributions are low, complicating the measurements.

The tactic we have chosen for improving the measurement precision is to use very long path lengths. Since the required straight-line path lengths are impractical in a laboratory setting, we have elected to “fold” these measurement paths with a device known as a White cell (named after the designer, J. U. White⁴).

EXPERIMENTAL CONFIGURATION

In previous measurements of the spectral cross section of *Bg* at APL,⁵ a short path length and an unstable platform contributed to unacceptable noise levels for the broadband transmissometer. To address these shortcomings, broadband and laser White cells were

constructed within the APL bio-aerosol chamber (Fig. 1). Each White cell consists of three identical 6-in.-dia. *f*/4 mirrors. In the broadband White cell, light from a fiber-coupled lamp (Cole-Parmer 9741-50) is brought to a focus with a 5× microscope objective next to the field mirror and allowed to expand to fill the first fold mirror. It is then focused onto the field mirror and expands again to fill the second fold mirror. After once more focusing onto the field mirror, the light repeats this sequence until the last reflection off the second fold mirror is focused with a 10× microscope objective onto an optical fiber that leads to an ultraviolet/near-infrared spectrometer (StellarNet EPP2000C). Output of the lamp is monitored with a silicon photodetector (Thorlabs PDA55) positioned near the output of the fiber (not shown).

Although the path length within the broadband transmissometer is significantly longer than that in previous measurements, it is still desirable to calibrate the broadband measurement with a laser transmissometer measurement. One reason for doing so is that the laser source offers significantly higher brightness and a smaller focused spot on the field mirror. Thus, longer path lengths can be achieved than with broadband sources. Another reason is that, to suppress background noise, the beam must be mechanically chopped and lock-in techniques used to measure the output power of the laser and the signal transmitted through the White cell. Since this cannot be accomplished easily with the current broadband system (the required integration time of the spectrometer does not allow the use of a modulated source), simultaneous laser measurements (with a HeNe laser at 543 nm) are made in a second White cell.

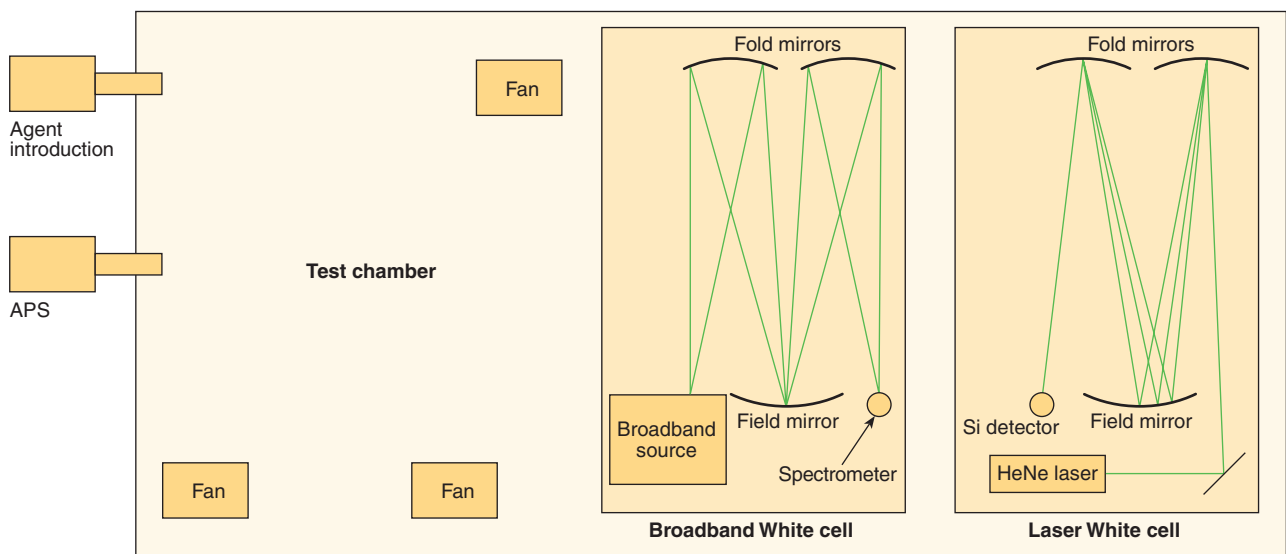


Figure 1. Experimental configuration in the APL bio-aerosol chamber. Particle size distribution and concentration are measured with an aerodynamic particle sizer (TSI Inc. Model APS 3320). (Figure not to scale.)

RESULTS

The broadband and laser transmissometers were operated simultaneously to measure the transmittance as the aerosol concentration was varied. Each laser transmittance value at 543 nm was calculated according to the formula

$$T = \frac{V_{\text{sig}}/V_{\text{ref}}}{V_{\text{sig}}^0/V_{\text{ref}}^0}, \quad (2)$$

where V_{sig} is the White cell signal detector voltage and V_{ref} is the laser reference detector voltage. Before introducing the aerosolized particles into the chamber, baseline voltages (V_{sig}^0 and V_{ref}^0) were recorded. All detector values were obtained by averaging data points collected every 0.7 s for 1 min. For each particle concentration level, quantities of *Bg* were introduced into the chamber and the mixture was allowed to stabilize for several minutes. Fans distributed the aerosol uniformly throughout the chamber.

The single-wavelength extinction coefficient was then estimated by using the relationship

$$\beta_{\text{ext}} = -\frac{1}{L} \ln(T), \quad (3)$$

where L is the path length of the transmissometer. For this test, a path length of 90 m was achieved with the White cell. Figure 2 shows the extinction coefficient as a function of *Bg* concentration. The measured data points are indicated in color, and the black curve represents a

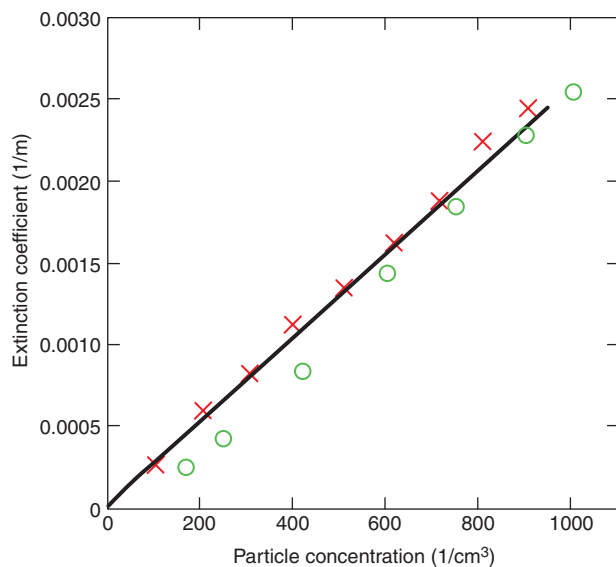


Figure 2. Experimental *Bg* extinction coefficient collected on two different dates (indicated in red and green) at 543 nm versus particle concentration. The line is the least-squares fit to the data and its slope is the extinction cross section, $C_{\text{ext}} = 2.58 \times 10^{-8} \text{ cm}^2$.

linear fit to these data. The extinction cross section is the slope of this curve as indicated by the relationship

$$C_{\text{ext}} = \frac{\beta_{\text{ext}}}{N}, \quad (4)$$

where N is the particle number density. For this set of measurements, the extinction cross section was estimated to be $2.58 (\pm 0.25) \times 10^{-8} \text{ cm}^2$. The observed variation could be caused by changes in the chamber's environmental condition (e.g., humidity), sample preparation, sample dissemination, and so on. Variations on a particular day are often within $\pm 2\%$.

Results from the laser transmissometer were used to calibrate the broadband laser transmissometer measurements. Figure 3 shows the spectral transmittance for different particle concentration levels. The laser calibration points at 543 nm are indicated by black boxes. Note that the transmittances are in the single scatter regime (see the boxed insert).

Several experimental spectrometer and laser spectral cross sections are plotted in Fig. 4, representing data over a 1-year period. Also shown is the corresponding Mie theory prediction.⁷ For this calculation, the bulk index of refraction was obtained from Tuminello et al.¹ Even though the computed extinction cross section is scaled by a factor of 1.2, agreement with the computed spectral shape is remarkably good. These spectra indicate little wavelength dependence throughout the visible. However, the cross section is expected to change dramatically as the wavelength increases, beginning in the near infrared.

Cross sections also depend on the particle size distribution of the aerosolized bacteria. Figure 5 shows a representative size distribution for *Bg* particles released into the aerosol chamber as measured by the APS. The

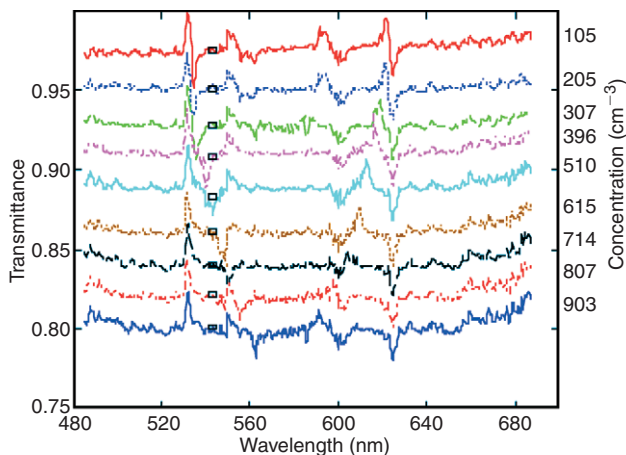


Figure 3. Transmittance versus wavelength for varying concentrations of *Bg*. Curves are broadband spectrometer results and boxes are laser results that calibrate the curves.

CONFLICTING MEASUREMENT REQUIREMENTS

In making estimates of the extinction of a propagation medium based on measurements of a beam propagating through it, we are faced with two conflicting requirements: (1) the transmission must be sufficiently high that we do not see any multiple scatter phenomena, but (2) it must be sufficiently low that the error in the estimate is not unduly influenced by errors in the measurement.

The basic measurement concept uses the so-called Bouguer-Lambert law.⁶ This is a model for attenuation due to scatter and absorption of a beam propagating through a medium of path length L . The relationship between the input intensity I_0 and the output intensity I is expressed as

$$I = I_0 e^{-\beta_{\text{ext}} L}, \quad (1)$$

where β_{ext} is the extinction per unit length or extinction cross section per unit volume. (It is often simply called the extinction “coefficient” but since it has the units of inverse length, it cannot be considered strictly a coefficient.)

Equation 1 is often expressed in terms of a transmittance,

$$T = \frac{I}{I_0} = e^{-\beta_{\text{ext}} L}. \quad (2)$$

This model for beam attenuation is predicated on the assumption of single scatter; i.e., it is assumed that in propagating a distance L , an individual photon is scattered, at most, one time. For the number of scatter events N , the probability of more than one scatter is given by

$$P(N > 1) = 1 - P(N \leq 1) = 1 - P(N = 0) - P(N = 1). \quad (3)$$

Treating the number of scatter events as a Poisson distributed phenomenon yields the probability of more than one scatter as

$$P(N > 1) = 1 - e^{-\beta L} - \beta L e^{-\beta L}. \quad (4)$$

From Eq. 4 we see that if we restrict our interest to situations in which the probability of more than one scatter is no more than 10%, then we must have a transmittance of no less than 0.59.

We next consider the competing requirement of a sufficiently low transmittance. The single particle extinction cross section is given by

$$C_{\text{ext}} = \frac{\beta_{\text{ext}}}{N}, \quad (5)$$

where N is the total number density per unit volume within the propagation medium. Equation 5, the relationship between extinction coefficient and concentration, is known as Beer’s law (Eq. 1 is often erroneously identified as such). If we combine Eqs. 2–5, we can determine the effect of measurement errors on the error in the estimate of the extinction cross section as

$$\frac{\Delta C_{\text{ext}}}{C_{\text{ext}}} = \frac{1}{\ln T} \frac{\Delta T}{T}, \quad (6)$$

where ΔT represents a small change in the measured transmittance and ΔC_{ext} the corresponding change in the estimated cross section.

Another way of expressing this relationship is in terms of signal-to-noise ratios:

$$\text{SNR}_{\text{estimate}} = |\ln T| \text{SNR}_{\text{measurement}}. \quad (7)$$

This result states that the error in the estimate is amplified by the error in the measurement. As an example, for a transmittance of 90%, a 30-dB measurement SNR yields a 3.16-dB estimate SNR. Put another way, a 2% measurement error produces a 19% uncertainty in the cross-section estimate.

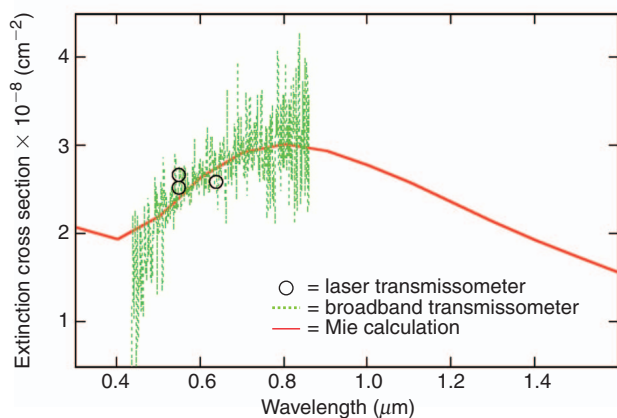


Figure 4. Spectral extinction cross section for B_g covering the visible and near infrared. Both long-path (90-m) and short-path (17-m) broadband measurements are plotted. The red curve is the Mie calculation scaled by 1.2.

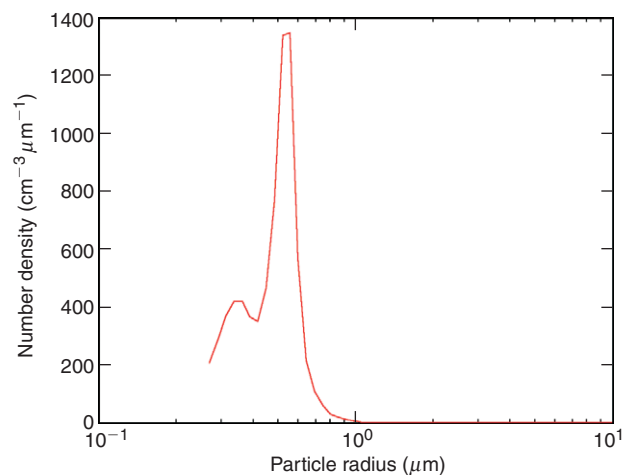


Figure 5. B_g particle size distribution function measured with the APS ($N = 565 \text{ cm}^{-3}$).

average effective diameter is about 1 μm . Note that the Bg particles are not spherical but more bean-shaped; however, since there is no preferred orientation of the particles, an assumption of a mean effective diameter sphere is not unreasonable. This supposition is borne out by Mie calculations that were performed assuming spherical particles.

DISCUSSION

Laser and broadband transmissometers using White cells built at APL demonstrate high SNR and stability. The data yield an extinction cross section of aerosolized Bg in the visible region of approximately $2.58 \times 10^{-8} \text{ cm}^2$. Mie theory calculations agree with the observed spectral shape of the extinction cross section but are lower in amplitude by a factor of about 1.2. These calculations require information on the complex refractive index of the aerosol constituent as well as the particle size distribution. Unfortunately, data on the refractive index of Bg are limited and of uncertain quality. In addition, there is some ambiguity in the specification of the equivalent spherical particle size distribution.

The APS device actually measures aerodynamic size⁸ rather than physical size. These two are related through the expression

$$d_a = d_e \left(\frac{\rho}{\rho_0 \chi} \right)^{\frac{1}{2}}, \quad (5)$$

where d_a and d_e are, respectively, the aerodynamic and equivalent volume diameters, ρ and ρ_0 are, respectively, the actual and reference densities (a reference density

equal to that of water is assumed, 1 g/cm^3), and χ is the dynamic shape parameter.

We assumed for Bg a cylinder of aspect ratio 2:1. For such a cylinder averaged over all orientations, $\chi = 1.09$. This shape parameter is larger for a more complex shape, so if particle agglomeration is an issue, there will be a greater disparity between particle size distribution as measured by the APS device and the physical particle size distribution as required for the Mie calculations. We are continuing to quantify these effects and bring measurements and calculations into agreement.

REFERENCES

- ¹Tuminello, S., Arakawa, E. T., Khare, B. N., Wrobel, J. M., Querry, M. R., and Milham, M. E., "Optical Properties of *Bacillus subtilis* Spores from 0.2 to 2.5 μm ," *Appl. Opt.* **36**, 2818–2814 (1997).
- ²Galica, G. E., Boies, M. T., Hinds, M., Krech, R., SADM, R., et al., "Development and Testing of a Tunable Infrared Lidar System for the Detection of Biological Aerosols via Differential Scattering," in *Proc. Fifth Joint Conf. on Standoff Detection for Chemical and Biological Defense*, CD-ROM (24–28 Sep 2001).
- ³Gurton, K. P., Ligon, D., and Kvavilashvili, R., "Measured Infrared Spectral Extinction for Aerosolized *Bacillus subtilis* var. *niger* Endospores from 3 to 13 μm ," *Appl. Opt.* **40**, 4443–4448 (2001).
- ⁴White, J. U., "Long Optical Paths of Large Aperture," *J. Opt. Soc. Am.* **32**, 285 (1942).
- ⁵Mitchell, C. A., Thomas, M. E., Walts, S. C., Duncan, D. D., Blodgett, D. W., et al., "Optical Characteristics of Airborne Bacteria," in *Proc. SPIE—Chemical and Biological Sensing III* **4722**, pp. 33–40 (1–5 Apr 2002).
- ⁶Hudson, R. D. Jr., *Infrared System Engineering*, John Wiley & Sons, New York (1969).
- ⁷Bohren, C. F., and Huffman, D. R., *Absorption and Scattering of Light by Small Particles*, Wiley-Interscience, New York (1983).
- ⁸TSI Inc. Web site, <http://www.tsi.com/> (accessed 13 Nov 2003).

ACKNOWLEDGMENT: The authors gratefully acknowledge the expert assistance of W. R. Drummond during the course of these experiments.

THE AUTHORS



SUZANNE C. WALTERS is an Associate Professional Staff engineer in the Electro-Optical Systems Group of APL's Air Defense Systems Department. She received a B.S. in physics from Wake Forest University in 1997 and an M.S. in electrical engineering from the University of Michigan in 1999. Since joining the Laboratory in 1999, Ms. Walts has been involved with measurements, data analysis, and modeling for various systems. Her research interests focus on materials characterization with optical methods. Her e-mail address is suzanne.walts@jhuapl.edu.



CRAIG A. MITCHELL is a member of the APL Senior Professional Staff. He received his B.S. degree in mechanical engineering from The University of Maryland, Baltimore County, in 1998. He joined APL in 1979 after working for AF&G Tool & Die in Baltimore, and is currently a mechanical engineer in the Electro-Optics Group of the Air Defense Systems Department. Mr. Mitchell has extensive experience in the manufacture of mechanical test hardware and numerically controlled machine tool programming. In 2003 he served as principal investigator for the Experimental Determination of Bacterial Aerosol Spectral Cross Section project. He is now working on several chemical and biological agent detection and characterization programs. His e-mail address is craig.mitchell@jhuapl.edu.



MICHAEL E. THOMAS received a B.E.E. degree from the University of Dayton and an M.S. and Ph.D. from The Ohio State University. Since joining APL in 1979, he has been working on electromagnetic propagation, optical properties of materials, and remote sensing. In 1982, he was a postdoctoral fellow in the Department of Physics at the Naval Postgraduate School. In 1988, Dr. Thomas became a faculty member of the JHU G.W.C. Whiting School of Engineering in the Part-Time Programs in Engineering and Applied Science, teaching courses on optical propagation and lasers. In 1998, he was appointed Research Professor in the Department of Electrical and Computer Engineering at JHU. His current research interests include experimental and theoretical modeling of atmospheric propagation in the infrared, optical and infrared window materials, lidar modeling, and femtosecond pulse propagation. Dr. Thomas is a fellow of the Optical Society of America. His e-mail address is michael.thomas@jhuapl.edu.



DONALD D. DUNCAN, a member of APL's Principal Professional Staff, received a Ph.D. in electrical engineering from Ohio State University in 1977. He is an Associate Professor of Ophthalmology at the Johns Hopkins School of Medicine and a lecturer in the JHU School of Continuing Education. From 1977 to 1983, Dr. Duncan was a senior analyst at the Pacific-Sierra Research Corporation in Santa Monica, California, conducting research in optical propagation through aerosol media and turbulence. He joined APL in 1983 and currently focuses on research projects in optics and biomedical engineering. He is the supervisor of the Phenomenology and Measurements Section in the Air Defense Systems Department's Electro-Optical Systems Group. His e-mail address is donald.duncan@jhuapl.edu.